Promoting effect of CeO$_2$ on cyclohexanol conversion over CeO$_2$–ZnO mixed oxide materials prepared by amorphous citrate process

BRAJA GOPAL MISHRA and G RANGA RAO*

Department of Chemistry, Indian Institute of Technology, Chennai 600 036, India

Abstract. CeO$_2$–ZnO materials were prepared by amorphous citrate process and characterized by TGA, XRD, UV–DRS and surface area measurements. TGA showed that the citrate precursors decompose in the range 350–550°C producing CeO$_2$-containing catalytic materials. XRD and DRS results indicated the formation of well-dispersed interstitial Zn$_x$Ce$^{4+}_{1-2x}$Ce$^{3+}_{2x}$O$_2$ solid solution on ZnO matrix. Addition of CeO$_2$ to ZnO produced high surface area mixed oxide materials in citrate method. Cyclohexanol conversion reaction was carried out on these catalytic materials to investigate the effect of rare earth oxide on the activity and selectivity. It was found that CeO$_2$ promotes the activity of ZnO without affecting the selectivity to cyclohexanone significantly. The factors such as reaction temperature and WHSV have turned out to be important for cyclohexanol conversion over CeO$_2$-containing ZnO catalyst materials.

Keywords. CeO$_2$–ZnO; cyclohexanol conversion; citrate process; acid-base properties.

1. Introduction

The dehydrogenation of cyclohexanol to cyclohexanone is a commercially important reaction in the production of caprolactam and has also been used as a good model reaction in probing acid-base properties of metal oxide materials (Bezouhanova and Al-Zihari 1991; Duprez and Martin 1997; Cesar et al 1999). Among various catalyst material formulations that have been studied for this reaction, CuO–ZnO has emerged to be the most effective oxide material with good conversion and selectivity for cyclohexanone at 673–723 K and atmospheric pressure (Okamoto et al 1983; Lin et al 1988; Sivaraj et al 1988; Bezouhanova and Al-Zihari 1991; Chen et al 1992; Duprez and Martin 1997; Cesar et al 1999; Fridman and Davydov 2000). This catalyst combination is also important for methanol synthesis and water–gas–shift reactions (Spencer 2000). The determination of the chemical nature of active copper species in these catalyst materials has been a subject of numerous investigations and a very recent study (Fridman and Davydov 2000) unambiguously concluded that zero and monovalent copper species constitute the active sites. The process of cyclohexanol conversion has also been studied using metal oxides from the first row transition metals, alkali and alkaline earth metals, bimetallic Cu–Co and Ni/C catalysts with an objective to evaluate the acid-base properties and promoting effects on the reaction (Bezouhanova and Al-Zihari 1991; Chen et al 1992; Duprez and Martin

1997; Cesar et al 1999). The process of cyclohexanol conversion leading to various products is summarized below:
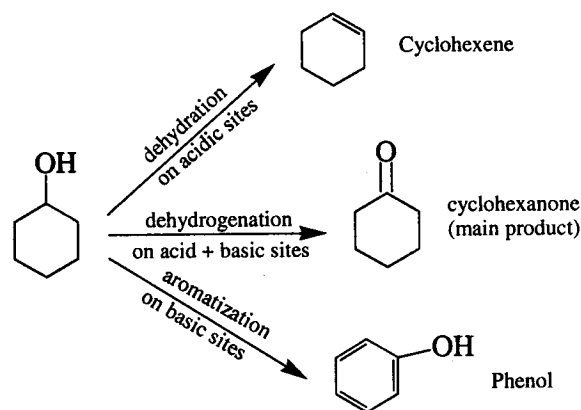
The preferred effect of a promoter on this reaction is to enhance the alcohol conversion at low temperatures with better product selectivity. It has been suggested that the dehydration of cyclohexanol leading to cyclohexene (C-ene) occur on acid sites while its dehydrogenation leading to cyclohexanone (C-one) is linked to both by acid and basic sites (Duprez and Martin 1997). Accordingly, the product ratio (C-one/C-ene) of cyclohexanol conversion could be used to evaluate the surface acid-base properties of various oxide materials. In general, dehydration takes place on acidic oxides such as V$_2$O$_5$, SiO$_2$–Al$_2$O$_3$ and sulfated-zirconia giving rise to cyclohexene as major product while on basic oxides such as MgO, ZnO

and CuO, dehydrogenation step is favoured leading to the formation of cyclohexanone as major product (Bezouhanova and Al-Zihari 1991; Duprez and Martin 1997). Aromatization of cyclohexanol producing small quantities of phenol has also been reported on CuO and NiO (Bezouhanova and Al-Zihari 1991; Fridman and Davydov 2000). However, there are no reports available in the literature investigating the effect of rare earth oxides on cyclohexanol conversion. Duprez and Martin (1997) reported that CeO_2 is more active for cyclohexanol conversion than pure MgO. Also MgO has higher selectivity towards cyclohexanone than CeO_2 due to its known basic character (basicity: MgO > CeO_2 > ZrO_2). Recently, CeO_2–MgO catalyst has been used to carry out ortho-selective methylation and propylation of phenol (Sato et al 1998, 1999). The redox property ($Ce^{3+} \rightleftharpoons Ce^{4+}$) and weak basicity of CeO_2 are said to be responsible for the activation of alkylating agent and overall higher catalytic activity. In another study, a ternary oxide system, CeO_2–AgO–V_2O_5, in which ceria is found to promote selective oxidation of toluene to benzaldehyde and benzoic acid (Yan and Andersson 1991). In addition to numerous organic transformations, ceria has been the key promoting oxide for CO oxidation and NO reduction reactions in exhaust catalysis (Ranga Rao et al 1996; Fornasiero et al 1998; Ranga Rao 1999; Li et al 2000).

The redox and acid-base properties of individual oxides can be tuned to produce surface acid-base and redox pair sites in mixed oxides to carry out organic reactions (Barteau 1996; Kabalka and Pagni 1997). Ceria is a strong redox promoter with mild acid-base properties and has been considered as a catalyst component for several organic transformations. The aim of the present study is to prepare CeO_2 dispersed ZnO materials and study the promoting effect of CeO_2 in ZnO matrix for cyclohexanol conversion. We have employed citrate method especially to obtain good dispersion of ceria promoter in ZnO matrix. It has been found that the cyclohexanol conversion activity is enhanced on CeO_2–ZnO materials and passed through a maximum as a function of CeO_2 content. The involvement of redox sites of ceria in the reaction is also demonstrated clearly.

2. Experimental

The mixed oxides of zinc and cerium were prepared by amorphous citrate process (Marcilly et al 1970). The CeO_2–ZnO of different compositions were prepared using cerium (III) nitrate hexahydrate ($Ce(NO_3)_3 \cdot 6H_2O$) (CDH chemicals), zinc nitrate hexahydrate ($Zn(NO_3)_2 \cdot 6H_2O$) and citric acid monohydrate ($C_6H_8O_7 \cdot H_2O$) (S.D. Fine Chemicals). A solid mixture of cerium and zinc nitrates of desired molar ratio was mixed with an equimolar amount of citric acid and heated at 70°C to form a uniform melt. The molten mixture was then evacuated at the same

temperature until it formed an expanded spongy solid material. It was then heated at 160°C for 2 h to decompose nitrates and calcined at 500°C for 2 h to obtain CeO_2–ZnO mixed oxide. Using this procedure we have prepared pure CeO_2, ZnO and CeO_2–ZnO mixed phases containing 20, 40, 60 and 80 mol% of CeO_2. The powder X-ray diffraction patterns of the samples were recorded using Philips X-ray diffractometer using Ni-filtered CuK_α radiation ($\lambda = 1.5418$ Å). Thermogravimetry analysis of citrate precursors was done on Perkin-Elmer TGA-7 apparatus in air (30 ml per min) with linear heating rate (20°C per min) from room temperature to 800°C. The specific surface areas were measured by BET method using Sorptomatic 1990 instrument at 77 K. The surface areas of the catalyst samples varied in the range 15–90 $m^2 g^{-1}$. UV-visible diffuse reflectance spectra of CeO_2–ZnO materials were recorded using Varian 5E spectrometer with $BaSO_4$ coated integration sphere. The samples were taken in the form of ~ 2 mm thick self supported pellets to measure the remission function $F(R_\infty)$.

The vapour phase dehydrogenation of cyclohexanol was carried out in a fixed bed flow glass reactor (i.d.: 2.2 cm, length: 30 cm) kept in a hot zone of a cylindrical furnace mounted vertically. Typically, 0.4 g of catalyst was loaded in the middle of the reactor and packed with clean glass beads. The temperature of the reaction was monitored by a thermocouple placed in the middle of the catalyst bed. Prior to the reaction, the catalyst was activated in an oxygen flow (20 ml/min) for 2 h at 450°C and then brought to the reaction temperature. Cyclohexanol (S.D. Fine Chemicals) was fed through the top of the reactor by means of a motor driven infusion pump (SP2S-MC model, Electronic Corporation, India). The liquid products were collected in an ice trap and analysed by gas chromatograph (AIMIL-Nucon 5765) using flame ionization detector and 20% carbowax column. The column temperature was controlled from 70 to 150°C at a linear heating rate of 10 K min^{-1}. Each reaction run continued for 1 h after initial equilibration period of 20 min. After each run the catalyst was reactivated at 450°C in oxygen for a subsequent run. Time-on-stream study of the catalysts was performed for a process time of 5 h.

3. Results and discussion

3.1 *TGA of Ce–Zn–O amorphous citrate precursor*

The CeO_2–ZnO mixed oxide catalysts were prepared by amorphous citrate process. This process has been used for the preparation of crystalline mixed oxides and oxide solid solutions of uniform composition and good dispersion (Marcilly et al 1970; Sato et al 1998). In citrate process, the precursor to a mixed metal oxide is an amorphous solid containing all required metal ions
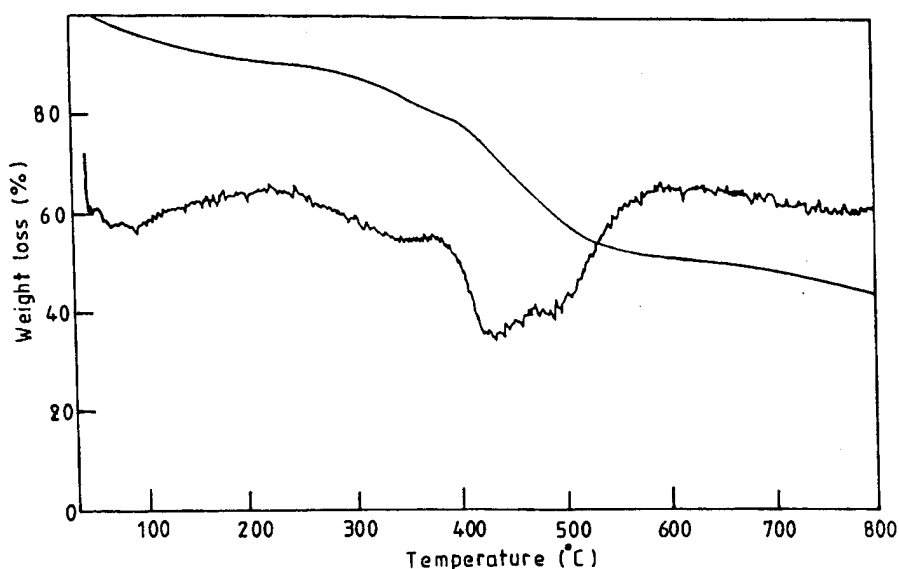
**Figure 1.** TGA curves for an amorphous citrate precursor in air (30 ml min⁻¹) at 20°C min⁻¹.

homogeneously mixed with a organic polyfunctional acid. It is prepared by rapid dehydration of a molten mixture or solution of metal salts under low pressure below 100°C. The key role of citric acid is to disperse the metal oxide components thoroughly. In the case of CeO₂–ZnO, the citrate process produced solid foam during dehydration and continued further expansion of the spongy material when heated in air at 160°C. The amorphous precursor showed uniform colouration indicating the atomic-level mixing of the constituent metal ions in the citrate process. Figure 1 shows the TGA curve of a typical amorphous precursor in air atmosphere. The corrugated line is the derivative of the smooth line. Crystalline CeO₂ with a wide range of porosity and high surface areas has been prepared by thermal decomposition of various cerium (III) and cerium (IV) salts in the temperature range of 300–600°C (Zaki and Sheppard 1983; Hussein 1996). In this work, the major weight loss is observed between 350 and 550°C which is attributed to the decomposition of citrate units and the formation of final oxide products containing CeO₂. The minor weight changes observed below 300°C are due to water loss from the hygroscopic precursors. Based on the TGA data, we have selected 500°C as the calcination temperature for all the citrate precursors in this study.

3.2 XRD profiles of CeO₂–ZnO materials

In figure 2, we present the X-ray diffraction profiles of the CeO₂–ZnO materials and the individual components prepared by amorphous citrate process. The X-ray reflections for ceria are observed at $2\theta = 28\cdot86$, $33\cdot41$, $47\cdot73$ and $56\cdot76$ corresponding to Miller indices of (111),
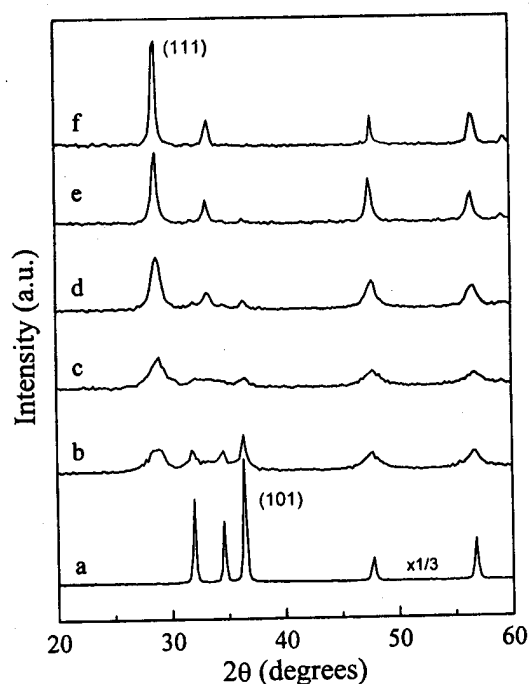
Figure 2. X-ray diffraction patterns for (a) ZnO, (b) CeO₂ (20%)–ZnO, (c) CeO₂(40%)–ZnO, (d) CeO₂(60%)–ZnO, (e) CeO₂ (80%)–ZnO and (f) CeO₂ samples prepared by amorphous citrate method.

(200), (220) and (311), respectively. Similarly the X-ray reflections for ZnO are observed at $2\theta = 32\cdot01$, $34\cdot65$, $36\cdot50$, $47\cdot74$ and $56\cdot80$ corresponding to the Miller indices of (100), (002), (101), (102) and (110), respectively. The diffraction peaks indicate that pure CeO₂ and ZnO samples are more crystalline compared to CeO₂–

ZnO mixed phase materials. The XRD profile of ZnO has been affected significantly due to the addition of 20% CeO_2. The diffraction pattern shows the formation of mixed oxide materials containing well-dispersed phases of semi-crystalline nature from both the constituent oxides. When ceria content is increased from 20% to 80% in the mixed oxide, the intensity of ZnO (101) peak decreased quite rapidly while the intensity of the CeO_2 (111) peak increased. In addition to the increase in intensity, the width of CeO_2 (111) peak decreased with ceria content, which indicates the growth of CeO_2 particles. However, XRD does not detect the ZnO phase beyond 40% of CeO_2 and clearly shows the fluorite phase of CeO_2 acting as a host lattice for ZnO. The fluorite (CaF_2) structure of CeO_2 consists of close-packed cubic structure of Ce^{4+} ions and O^{2-} ions occupy all the tetrahedral holes. All the octahedral holes remain vacant. Since X-ray diffraction pattern do not indicate any change in the lattice parameter of fluorite phase CeO_2, the disappearance of ZnO phase at higher CeO_2 contents can be attributed to the insertion of Zn^{2+} ions into the large vacant octahedral holes in CeO_2 crystallites. This is possible because of the smaller ionic radius of Zn^{2+} $(0.74$ Å$)$ compared to that of Ce^{4+} $(0.94$ Å$)$. The formation of a substitutional solid solution in this case is not expected because of large difference in ionic radii of Ce and Zn. However, fluorite type substitutional solid solutions are known for systems like CeO_2–ZrO_2 and CeO_2–Mn_2O_3 due to the structural similarities of the constituents (Trovarelli *et al* 1997; Machida *et al* 2001). If Ce^{4+} ions in the fluorite lattice were substituted by Zn^{2+} ions, there should be a change in the 2θ values of the diffraction peaks in figure 2 affecting the lattice constant which is normally observed in the substitutional solid solutions like CeO_2–ZrO_2. Insertion of smaller cations such as Mg^{2+} $(0.72$ Å$)$, which is comparable to that of Zn^{2+}, into the interstitial positions of CeO_2 lattice forming a nonequilibrium solid solution has been reported in the case of CeO_2–MgO catalyst material (Sato *et al* 1998). Citrate process seems to be effective to obtain such systems at low temperatures (Nakayama *et al* 1997; Sato *et al* 1998). From the above discussion, we can arrive at the conclusion that CeO_2–ZnO materials prepared by amorphous citrate method consist of well-dispersed CeO_2 and interstitial solid solution, $Zn_xCe^{4+}_{1-2x}$ $Ce^{3+}_{2x}O_2$ in ZnO matrix.

3.3 *UV-visible diffuse reflectance study of CeO_2–ZnO materials*

UV–DRS has been extensively used to characterize the nature of nano-sized oxide particles (Bensalem *et al* 1992; Weckhuysen and Schoonheydt 1999; Ranga Rao and Sahu 2001). The UV absorption edge wavelength is very sensitive to the particle size of semiconductor materials

such as ceria. When crystallite size of CeO_2 is below 10 nm, the band gap energy is inversely related to the crystallite size and the absorption edge of interband transition is blue shifted. Such blue shifts of the interband transition energy (i.e. band gap) are clearly seen in the UV region of DRS for very small ceria particles of 1–5 nm size (Bensalem *et al* 1995). In addition to blue shift, DRS shows four narrow bands in the range 250–350 nm for small CeO_2 crystallites $(< 2$ nm$)$ and can detect <100 ppm of cerium in a supported powder catalyst. These bands are attributed to localized O–Ce charge transfer transitions involving a number of surface Ce^{4+} ions with different coordination numbers (Bensalem *et al* 1995). The coordination number of surface Ce^{4+} ion can vary between four and eight, the latter being the coordination number of bulk Ce^{4+}.

In figure 3, we have shown the DRS spectra of CeO_2–ZnO materials which exhibited higher activities in cyclohexanol conversion (discussed in the following sections). These spectra show the characteristic strong absorption in the UV range (below 400 nm) superimposed by several smaller peaks due to localized transitions (Bensalem *et al* 1995; Ranga Rao and Sahu 2001). These small features indicate that CeO_2 is well dispersed in CeO_2–ZnO
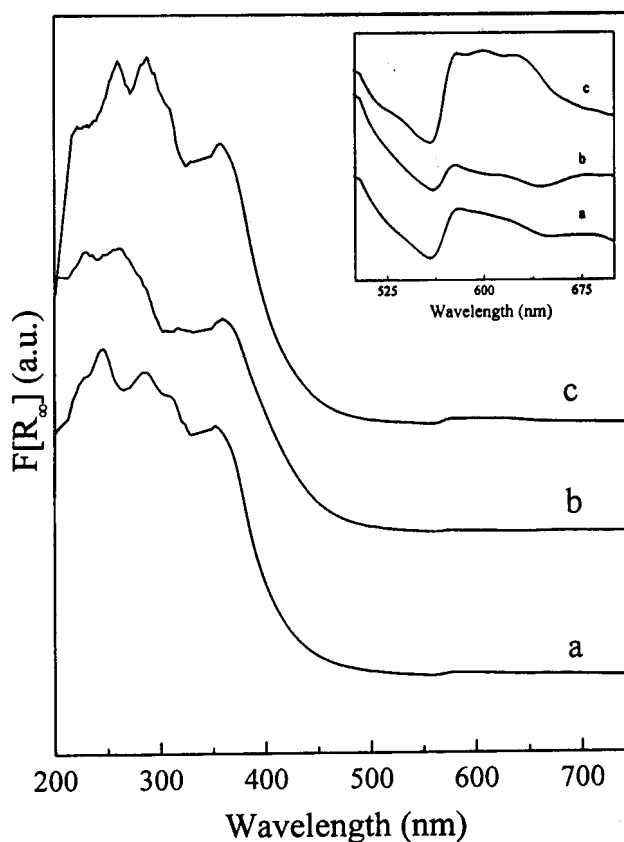
Figure 3. The UV–DRS spectra of (a) CeO_2 (60%)–ZnO, (b) CeO_2 (40%)–ZnO and (c) CeO_2 (20%)–ZnO. Inset shows the portion of DRS in the range 500–700 nm.

materials prepared by citrate precursor method. The inset in figure 3 shows a broad feature between 570 and 640 nm which is attributed to reduced CeO_2 on the surface ($Ce^{3+} \rightarrow Ce^{4+}$) of the particles (Binet *et al* 1994). It is evident that the citrate method produces well-dispersed nanosize-CeO_2 particles containing low coordinated surface Ce^{4+} and Ce^{3+} ions.

3.4 *Effect of ceria on cyclohexanol conversion*

Cyclohexanol conversion reaction over CeO_2–ZnO materials was carried out in vapour phase in the temperature range 325–400°C. Table 1 summarizes the catalytic conversion results on various CeO_2–ZnO catalysts at 400°C and WHSV 9·50 h⁻¹ along with surface area. The product collected initially for about 20 min was discarded in order to reach the equilibrium conversions. The conversions reported in table 1 are the average conversions obtained over 1 h. ZnO shows about 62% conversion and 97% selectivity to cyclohexanone. However, addition of CeO_2 component enhances the activity of the catalyst and the average conversions reach maximum at 40% CeO_2 content. The activity enhancement can as well be correlated with the increase in surface area of the materials, particularly those with high ZnO content (table 1). There

is, however, a marginal decrease in selectivity to cyclohexanone by about 6% compared to that of pure ZnO while the selectivity to cyclohexene is always small except on pure CeO_2 (43%). As previously mentioned, the dehydration of cyclohexanol to cyclohexene on acidic sites and dehydrogenation of cyclohexanol to cyclohexanone on acid-base sites can be taken as a qualitative measure of the availability of particular sites on oxide catalysts (Duprez and Martin 1997). From product selectivity values in table 1, we can see that CeO_2 contains nearly equal distribution of both acidic and basic sites while ZnO mainly exposes strong basic sites to the reactant molecules. ZnO is a known solid base with some acidic nature (Knoezinger 1976; Cardona-Martinez and Dumesic 1991) while CeO_2 seems to exhibit weak basic and acidic properties (Zaki and Sheppard 1983; Choudhary and Rane 1991; Käßner and Baerns 1996; Sato *et al* 1999). It is, therefore, expected that ceria addition to ZnO and *vice versa* could increase the total number of basic sites and also contributes weak acidic sites to CeO_2–ZnO catalyst. It is, therefore, speculated that CeO_2-containing ZnO catalyst provides the required number of acid-base properties to catalyze the reaction with high conversions in the dehydrogenation pathway leading to the main product cyclohexanone. Accordingly,

Table 1. Conversion and product selectivity with ceria (mol%) content in CeO_2–ZnO catalysts at 400°C.

Catalyst	Surface area (m²/g)	Cyclohexanol conversion (mol%)	Selectivity (%)	
			Cyclohexanone	Cyclohexene
ZnO	15·4	62·4	97·1	2·9
CeO₂(20%)–ZnO	35·6	75·8	86·0	14·0
CeO₂(40%)–ZnO	59·9	86·0	90·5	9·5
CeO₂(60%)–ZnO	90·7	71·3	85·4	14·6
CeO₂(80%)–ZnO	30·6	69·6	83·2	16·8
CeO₂	34·2	26·1	56·7	43·3

Table 2. Cyclohexanol conversion over CeO_2–ZnO catalysts.

Catalyst	Reaction temperature (°C)	Conversion of cyclohexanol (mol%)	Selectivity (mol%)	
			Cyclohexanone	Cyclohexene
ZnO	325	15·6	96·6	3·4
ZnO	350	34·5	96·9	3·1
ZnO	375	50·6	96·7	3·3
ZnO	400	62·4	97·1	2·9
CeO₂(40%)–ZnO	325	38·5	93·8	6·2
CeO₂(40%)–ZnO	350	50·7	91·9	8·1
CeO₂(40%)–ZnO	375	64·2	92·5	7·5
CeO₂(40%)–ZnO	400	84·2	90·5	9·5
CeO₂	325	6·5	90·7	9·3
CeO₂	350	8·6	75·3	24·7
CeO₂	375	12·5	68·4	31·6
CeO₂	400	26·1	56·6	43·4

the conversion of cyclohexanol increased with increasing CeO_2 content and the selectivity to cyclohexanone decreased only slightly. As shown in table 1, the cyclohexanol conversion rates are high in general in CeO_2-containing catalysts which agrees well with the concerted mechanism involving both acid-base sites proposed by Duprez and Martin (1997).

Sato and co-workers also reported similar reactivity trend for phenol alkylation on CeO_2-MgO catalysts with maximum phenol conversion at 11·2 mol% of CeO_2 in MgO. The alkylation reaction was proposed to involve the redox property of CeO_2 and acid-base sites on CeO_2–MgO. In the present study, incorporation of Zn^{2+} ions in the interstitial positions can modify the morphology of the catalyst and expose low coordinated cations of Ce and Zn which can function as Lewis acid sites at the surface. The UV–DRS study provides evidence for the existence of such low coordinated Ce ions on the surface of the catalyst particles. Here the charge/radius ratio for Ce^{4+} turns out to be 4·26 and for Zn^{2+} it is 2·70. Therefore Ce^{4+}–O is expected to be more covalent than Zn^{2+}–O. Accordingly, CeO_2 will have more acidic sites than ZnO. In other words, ZnO with its lower charge/radius ratio is more ionic and would exhibit higher basic sites. This method of predicting the relative acidic and basic nature is also consistent with the product selectivity results in table 1. However, in CeO_2–ZnO, Ce^{4+} ions of different degrees of coordination unsaturation will act as Lewis acidic sites and the associated O^{2-} ions behave like Brønsted base sites for cyclohexanol dehydrogenation reaction. The Ce^{4+} ions present in CeO_2–ZnO catalyst are more Lewis acidic than Zn^{2+} ions. The dehydrogenation centres in the CeO_2–ZnO are essentially the coordinately unsaturated Ce^{4+}–O^{2-} pair sites. Based on these considerations, we propose the following as one of the possible mechanisms by which CeO_2 can act as promoter enhancing the cyclohexanol conversions:
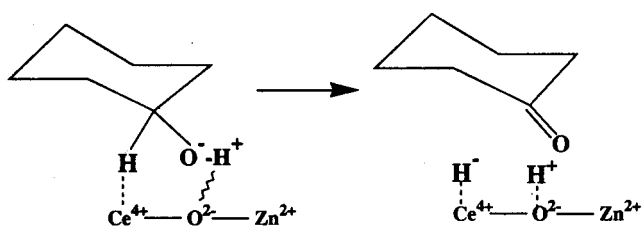
Walker and Lambert (1992) have reported a reaction between hydrogen and cerium forming cerium hydride phases. Taking this observation and also the redox nature of cerium ion into account, we conclude that the abstraction of hydride ion is more efficient at the Ce^{4+} ion (Lewis acid) site than Zn^{2+} ion site in the CeO_2–ZnO mixed oxide·catalyst. This reaction pathway can also contribute to higher cyclohexanol conversions and explain the high selectivity to cyclohexanone.

3.5 *Effect of temperature*

We have studied the effect of reaction temperature (325–400°C) on cyclohexanol conversion over CeO_2, ZnO and CeO_2(40%)–ZnO catalysts and the results are summarized in table 2. The overall conversion of cyclohexanol showed an increasing trend with an increase in reaction temperature for all three catalysts. A maximum of 84·2% cyclohexanol conversion was obtained again on CeO_2 (40%)–ZnO with same product distribution at 400°C (table 1). However, the selectivity for cyclohexanone and cyclohexene did not change significantly in the case of ZnO, while there was a drastic decrease in selectivity for cyclohexanone from 90·7% to 56·6% and an increase in selectivity for cyclohexene from 9·3% to 43·4% on CeO_2. It is important to note that even though cyclohexanol conversion is very less (6·5%) at 325°C on CeO_2, the selectivity for cyclohexanone is very high and comparable to that of ZnO and CeO_2–ZnO catalysts. It is, therefore, evident that CeO_2 clearly promotes cyclohexanol conversion at higher temperatures and also maintains higher selectivity for cyclohexanone.

3.6 *Effect of WHSV*

The transformation of cyclohexanol was carried out from 9·5 h^{-1} to 28·5 h^{-1} WHSV at 400°C on CeO_2, CeO_2 (40%)–ZnO and ZnO. The results are presented in table 3. It can be seen from table 3 that the cyclohexanol conversion decreased with an increase in the WHSV on all catalysts and a comparison of the activities of the three catalysts shows that for a given space velocity, CeO_2 (40%)–ZnO is more active than its constituent oxides throughout the range of WHSV studied. The decrease in conversion with WHSV is more rapid for ZnO from 62·4% to 34·7% and for CeO_2(40%)–ZnO from 84·2% to 49·6%. However, the selectivity showed little dependence on WHSV in all the three catalysts (table 3). Generally, a decrease in the conversion is observed at higher space velocities due to lesser contact time and kinetics may get affected to a certain extent. The results of the present study indicate that to maintain higher activity and good selectivity to cyclohexanone, the reaction should be carried out at lower WHSV and higher temperature, between 325 and 400°C.

3.7 *Time on stream*

Figure 4 shows the effect of reaction time on the activity of CeO_2, CeO_2(40%)–ZnO and ZnO catalysts studied by carrying out the cyclohexanol conversion reaction continuously for 5 h at 400°C and a space velocity of 9·5 h^{-1}. Firstly, among all the three catalysts, CeO_2(40%)–ZnO shows the highest activity following ZnO. The reaction seems to attain the steady state condition rather quickly

Table 3. Cyclohexanol conversion and selectivity values over CeO_2–ZnO catalysts at various WHSV (h^{-1}) and 400°C.

WHSV (h^{-1})	CeO₂			ZnO			CeO₂(40%)–ZnO		
	Conversion (mol%)	Selectivity (%)		Conversion (mol%)	Selectivity (%)		Conversion (mol%)	Selectivity (%)	
		1	2		1	2		1	2
09·50	25·9	56·6	43·4	62·4	97·1	2·9	84·2	90·5	9·5
14·25	22·6	64·9	35·1	54·3	97·3	2·7	77·2	92·2	7·8
19·00	19·7	62·7	37·3	48·8	96·7	3·3	63·6	92·7	7·3
23·75	18·1	64·0	36·0	42·6	96·9	3·1	54·2	93·7	6·3
28·50	16·3	61·4	38·6	34·7	97·0	3·0	49·6	93·2	6·8

1 = Cyclohexanone; 2 = cyclohexene.
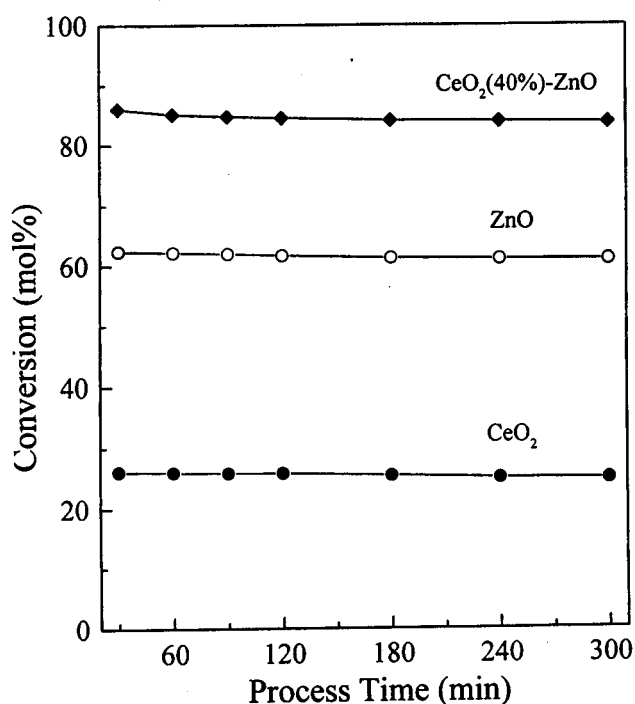
Figure 4. Cyclohexanol conversion with process time over CeO₂, ZnO and CeO₂(40%)–ZnO catalysts.

and there is no significant deactivation observed except that CeO₂-containing catalyst shows a marginal decrease of about 3% in the conversion activity at the end of the fifth hour of the study. The negligible deactivation of the catalysts may be attributed to the citrate process by which highly active and well-dispersed catalysts can be prepared.

4. Conclusions

Amorphous citrate process yields a well-dispersed CeO₂–ZnO catalyst. Based on XRD and DRS results, the formation of interstitial solid solution of $Zn_xCe^{4+}_{1-2x}Ce^{3+}_{2x}O_2$ phase on ZnO matrix is speculated. DRS results indicate the presence of Ce^{4+} and Ce^{3+} ions in various coordina-

tion sites on finely dispersed particles. CeO₂-containing catalysts are more active for cyclohexanol conversion which passes through a maximum at 40% CeO₂ content. The activity of CeO₂–ZnO catalysts compared to ZnO and CeO₂ is higher at lower values of space velocity and temperature (325°C) for cyclohexanol conversion. CeO₂ in ZnO promotes cyclohexanol conversion with more than 90% selectivity to cyclohexanone. The mechanism involving Ce^{4+} sites in the cyclohexanol conversion reaction has been proposed.

Acknowledgements

References

Barteau M A 1996 *Chem. Rev.* **96** 1413
Bensalem A, Muller J C and Bozon-Verduraz F 1992 *J. Chem. Soc. Faraday Trans.* **88** 153
Bensalem A, Bozon-Verduraz F, Delamar M and Bugli G 1995 *Appl. Catal. A: Gen.* **121** 81
Bezouhanova C P and Al-Zihari M A 1991 *Catal. Letts* **11** 245
Binet C, Bardi A and Lavalley J C 1994 *J. Phys. Chem.* **98** 6392
Cardona-Martinez N and Dumesic J A 1991 *J. Catal.* **127** 706
Cesar D A, Peréz C A, Salim V M M and Schmal M 1999 *Appl. Catal. A: Gen.* **176** 205
Chen W, Lee M and Lee J 1992 *Appl. Catal. A: Gen.* **83** 201
Choudhary V R and Rane V H 1991 *J. Catal.* **130** 411
Duprez D and Martin D 1997 *J. Mol. Catal. A: Chem.* **118** 113
Fornasiero P, Ranga Rao G, Kasper J, 'Erario F L and Graziani M 1998 *J. Catal.* **175** 269
Fridman V Z and Davydov A A 2000 *J. Catal.* **195** 20
Hussein G A M 1996 *J. Anal. Appl. Pyrolysis* **37** 111
Kabalka G W and Pagni R M 1997 *Tetrahedron* **53** 7999
Käßner P and Baerns M 1996 *Appl. Catal. A: Gen.* **139** 107
Knoezinger H 1976 *Adv. Catal.* **25** 184

Li Y, Fu Q and Flytzani-Stephanopoulos M 2000 *Appl. Catal. B. Environ.* **27** 179

Lin Y, Wang I and Yeh C 1988 *Appl. Catal.* **41** 53

Machida M, Uto M, Kurogi D and Kijima T 2001 *J. Mater. Chem.* **11** 900

Marcilly C, Courty P and Delmon B 1970 *J. Am. Ceram. Soc.* **53** 56

Nakayama T, Ichikuni N, Sato S and Nozaki F 1997 *Appl. Catal.* **A158** 185

Okamoto Y, Fukino K, Imanaka T and Teranlchi S 1983 *J. Phys. Chem.* **87** 3747

Ranga Rao G 1999 *Bull. Mater. Sci.* **22** 89

Ranga Rao G and Sahu H R 2001 *Proc. Indian Acad. Sci. (Chem. Sci.)* **113** 651

Ranga Rao G *et al* 1996 *J. Catal.* **162** 1

Sato S, Koizumi K and Nozaki F 1998 *J. Catal.* **178** 264

Sato S, Takahasi R, Sodesawa T, Matsumoto K and Kamimura Y 1999 *J. Catal.* **184** 180

Sivaraj Ch, Reddy B M and Kanta Rao P 1988 *J. Mol. Catal.* **47** 17

Spencer M S 2000 *Catal. Letts* **66** 255

Trovarelli A, Zamar F, Llorca J, Leitenburg C, Dolcetti G and Kiss J T 1997 *J. Catal.* **169** 490

Walker A P and Lambert R M 1992 *J. Phys. Chem.* **96** 2265

Weckhuysen B W and Schoonheydt R A 1999 *Catal. Today* **49** 441

Yan Z G and Andersson S L T 1991 *J. Catal.* **131** 350

Zaki M I and Sheppard N 1983 *J. Catal.* **80** 114